Arch. Mech., 35, 5–6, pp. 591–601, Warszawa 1983

A study of plastic strain processes in PA4 aluminium alloy

T. BRECZKO (BIAŁYSTOK)

THE PRESENT PAPER discusses the measurement results obtained for the principal directions of the plastic strain tensor and the residual macrostress tensor. The grid method was used for analysis, the stress measurement being performed by the X-ray technique. Other results presented here and obtained by the X-ray technique are those of measurement of residual microstresses. The analysis shows that the displacement of the yield surface in the space of stresses is due to the residual microstress field.

W pracy przedstawiono wyniki pomiarów kierunków głównych tensora odkształceń plastycznych oraz tensora makronaprężeń szczątkowych. Do badań stosowano metodę siatek oraz metodę rentgenowską pomiaru naprężeń. Przedstawiono również wyniki pomiarów metodą rentgenowską mikronaprężeń szczątkowych. Wyniki badań wskazują, że przemieszczenie się powierzchni plastyczności w przestrzeni naprężeń jest spowodowane polem mikronaprężeń szczątkowych.

В работе представлены результаты измерений главных направлений тензора пластических деформаций, а также тензора остаточных макронапряжений. Для исследований применен метод сеток и рентгеновский метод измерения напряжений. Представлены тоже результаты измерений рентгеновским методом остаточных микронапряжений. Результаты исследований указывают, что перемещение поверхности пластичности в пространстве напряжений вызвано полем остаточных микронапряжений.

1. Introduction

THE PROBLEM of strain hardening of polycrystalline materials plays a very important role in the theory of plasticity. To describe the Bauschinger effect, a theory of kinematic hardening was introduced by A. J. ISHLINSKY [1], W. PRAGER [2] and R. T. SHIELD and H. ZIEGLER [3]. According to the idea of J. I. KADASHEVITCH and V. V. NOVOZHILOV [4], the yield surface is displaced as a result of strain hardening and expands in a uniform manner, the geometric similarity being preserved. On the basis of an experimental analysis by J. MIASTKOWSKI and W. SZCZEPIŃSKI [6], a strain hardening law was put forward by A. BAŁTOW and A. SAWCZUK [5], in which the rotation of the yield surface was taken into account.

If a monocrystal is subjected to plastic strain, slips occur in densely spaced crystallographic planes in close-packed directions. The slips depend on the shear stresses in the slip planes and are independent of the normal stresses. Much attention was devoted to experimental stress-strain relations obtained for monocrystals with a view to establish laws of plastic flow in polycrystalline bodies. The principal difference between monocrystals and polycrystals is that there are grain boundaries in the latter bodies. Neighbouring grains being oriented in a different manner, plastic strain is constrained. In mono-

crystals formed in a regular system of face centered crystal lattice, there occur two systems of slips, that is $\{111\}\langle\bar{1}01\rangle$ and $\{010\}\langle\bar{1}01\rangle$. Plastic strain of a particular grain depends on the orientation of its plane and the direction of easy slip with reference to that of the stress. Grains oriented with reference to the stress in a more favourable manner undergo greater deformation than other grains. If the external load is removed, plastically deformed grains produce elastic strain in the neighbouring grains, the latter acting in turn on the former, which undergo elastic strain. Plastic deformation produces defects, about which stress fields are generated. These stresses are equilibrated within regions, the size of which is of the order of a few scores to a few hundreds of interatomic distances. They are stresses of the third kind $\sigma^{(3)}$ or static deformations of the crystal lattice (Fig. 1). The components of the stress field equilibrated within the region of one or several blocks are termed stresses of the second kind $\sigma^{(2)}$ (Fig. 1). The quantities measured are, in prac-

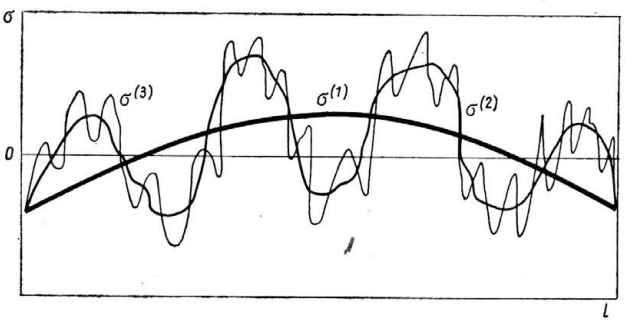

FIG. 1. Classification of residual stresses: $\sigma^{(1)}$ — macrostresses, $\sigma^{(2)}$ — microstresses, $\sigma^{(3)}$ — static deformation of the crystal lattice (stress of the 3-rd kind).

tice, the quadratic means of the relevant distortion of the crystal lattice. This quantity can be defined as a ratio of the quadratic mean of the increase in the measurement length L to that length itself: $\sqrt{\langle\varepsilon\rangle^2} = \sqrt{\Delta L^2}/L$. Stresses of the second kind are also referred to as residual microstresses. The components $\sigma^{(1)}$ (Fig. 1) of the stress field which are equilibrated within the object as a whole are referred to as stresses of the first kind or residual macrostresses.

2. The material and the test pieces

PA4 (Al Mg Si Mn) aluminium alloy was used for tests. Large 100×500 mm plane test pieces were cut out from a 5 mm sheet in the direction of rolling and subjected to soft annealing, that is to soaking at a temperature of 350°C, for 180 minutes, followed by cooling in a furnace. As a result of annealing, Mg_2Si was completely separated from the oversaturated Mg_2Si solution in Al [7]. This made the Guinier–Preston zones disintegrate, the material thus losing its properties acquired during dispersion hardening. This is proved by the yield limit being low after annealing (Fig. 3).

2.1. Verification for isotropy

To verify the annealed test pieces for isotropy, seven small test pieces were cut out from one of them at an angle $\alpha = 0.15, 30, 45, 60, 75$ and $90°$ with reference to the direction of rolling (Fig. 2). The dimensions of those test pieces were 10 mm in width and 100 mm in length. They were subjected to uniaxial tension, the stress being determined for plastic strains $\varepsilon_{pl} = 0.2$ and 0.5%. The measurement results are represented in the form of yield

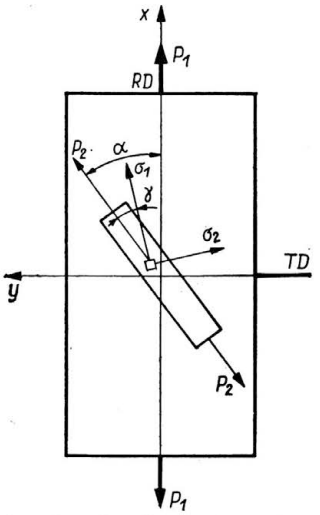

FIG. 2. Directions of strain: P_1 — direction of prestraining, P_2 — direction of secondary tension.

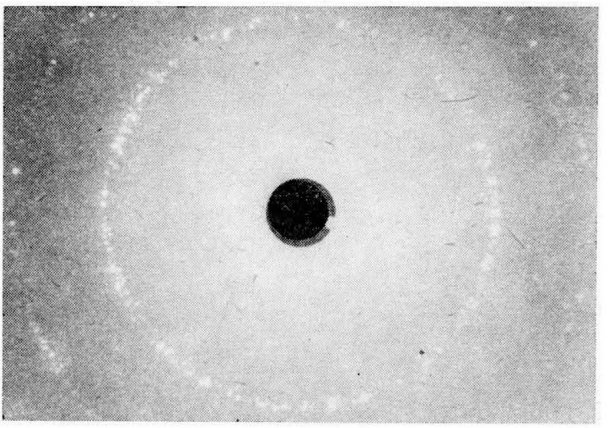

FIG. 3. Back reflection photograph of PA4 alloy normalized 2 hr at 350°C.

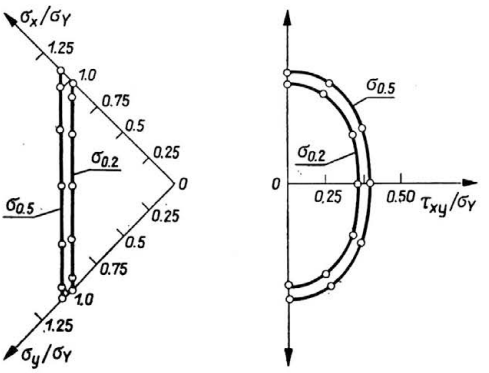

FIG. 4. Curves representing the yield surface of the PA4 alloy after soft annealing.

surfaces in the σ_x, σ_y, τ_{xy}-space of stresses (Fig. 4) [8]. Another small test piece was cut out from the annealed specimen and polished. It was used for determining the texture of the surface of the plate and for obtaining an X-ray diffraction image by the method of back-reflection radiation. A diffraction photograph was made with a plane-cassette camera making use of nonfiltrated CuKα radiation. The incident beam was 0.5 mm in

diameter. The diffraction photograph is represented in Fig. 3. The incomplete polar figure of {111} planes, representing the texture of the surface of the plate, shown in Fig. 5, was taken with a DRON-1.5 X-ray diffractometer. The method of reflected CuKα radiation was used for analysis. From Fig. 3 it is seen that the grain size of the PA4 alloy plate used for the tests was greater than 10^{-3} cm. This is proved by the Laue spots forming the trace of the Debye ring. The small difference of pole density of {111} planes, which can be seen in the polar figure (Fig. 5), is due to the grain size being rather large, not to the texture. Thus the texture of the PA4 alloy used for tests did not entail anisotropy of plastic properties, which is proved by the symmetry of the yield surface represented in Fig. 4.

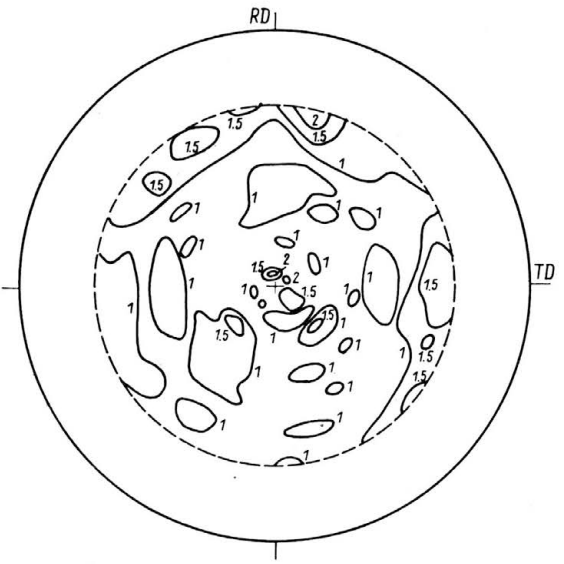

FIG. 5. The polar figure of planes {111} representing the texture of the surface of a PA4 alloy normalized 2.5 hr at 350°C.

3. Experimental analysis of plastic strain

The subject of the analysis was the variation of the deviation angle γ of the principal direction of the plastic strain tensor from the direction of tension of a test piece cut out from a specimen which had been subjected to previous plastic strain. The angle γ was evaluated by the grid method. To this aim 2 mm square meshes were drawn on the surface of a large specimen which was then subjected to initial 10% plastic strain in the direction of rolling. Two 10×100 mm test pieces were cut out from the strained specimen for each of the angles $\alpha = 0$, 30, 60 and 90° with the x-axis (Fig. 2) parallel to the direction of rolling. One group of test pieces cut out at different angles was subjected to uniaxial tension to produce a strain $\varepsilon_p = 5\%$, the other group being tensioned up to $\varepsilon_p = 10\%$. Then the coordinates of the eight nodes surrounding the three nodes selected for each specimen (Fig. 6) were measured. The computation work was carried out on the ODRA-1204 computer, making use of a program written by the present author. The

algorithm used was based on an approximation by polynomials to the relation between the initial coordinates y_k and the current coordinates x_k^i of the selected nodes [9]

$$y_k = A_{kij} x_k^i x_k^j \quad (k = 1, 2), \quad (i, j = 0, 1). \tag{3.1}$$

First degree polynomials were assumed for computation $(i, j = 0.1)$, the method of least squares being used [9].

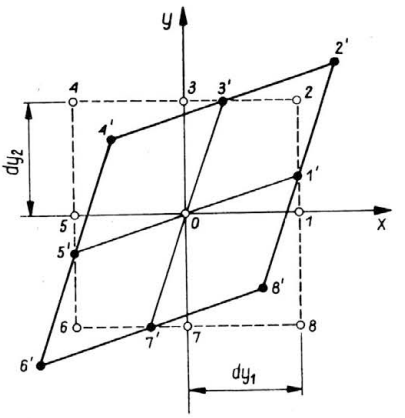

FIG. 6. Coordinates of grid nodes.

Experimental investigation showed that the value of the Poisson's ratio ν depends on the stress [10]. With increasing stress, ν first decreases, for pure aluminium, then increases up to a value higher than 0.46 [10]. On the basis of the results of that reference and the work of G. D. DIEL [9], it was assumed that the material is incompressible ($\nu = 0.5$) in the course of a plastic process. This enables us to make the values of the coefficients of the polynomials (3.1) more accurate, using the condition of incompressibility for plane strain(1) [9]

$$\left| \frac{\partial y_k}{\partial x_l} \right| = 1. \tag{3.2}$$

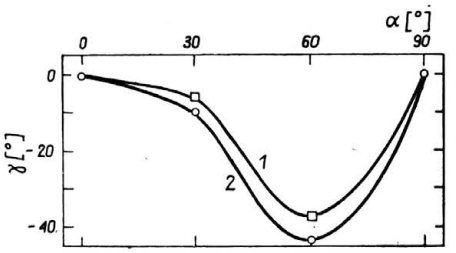

FIG. 7. Variation of the angle γ between the proper direction of the strain tensor and the direction of the secondary plastic strain of test pieces cut out at an angle α with the direction of prestrain to $\varepsilon_p^{\mathrm{I}} = 10\%$, $1 - \varepsilon_p^{\mathrm{II}} = 10\%$, $2 - \varepsilon_p^{\mathrm{II}} = 5\%$.

(1) Replacement of the incompressibility condition (3.2) with the relevant condition for plane stress does not introduce, in the case considered, any essential change in the value of the angle 2β (Eq. (3.3)).

The double angle between the x-axis of the large specimen and the proper direction of plastic strain in a test piece after the second straining operation was calculated from the formula [9]

$$2\beta = \arctan\left(2(A_{110}A_{101}+A_{210}A_{201})/(A_{101}^2+A_{201}^2-A_{110}^2-A_{210}^2)\right). \tag{3.3}$$

The results of computation for the angle

$$\gamma = \beta-\alpha \tag{3.4}$$

are represented in Fig. 7.

4. Experimental investigation into the residual macrostress

Many authors found, by experimental means, that a residual stress field is produced as a result of uniaxial plastic strain in the upper layer of the test-piece, the sign of that stress field being opposite to that of the external stress producing the plastic strain. The problem of generation of a residual stress field as a result of plastic strain was studied in the early forties by W. A. Word and S. L. Smith who attempted to explain the physical nature and the causes of occurrence of residual stresses. Their theory of residual plastic strain of a crystal lattice was criticized by N. N. DAVIDENKOV and E. L. ASSUR [16] who proved experimentally, in 1949, that the stress field in middle layers of a test piece subjected to uniaxial tension takes a sign which is opposite to that of the stress in the surface layer. By the same it was proved that the stresses observed experimentally are equilibrated over the cross-section of the test-piece, therefore they constitute residual macrostresses. N. N. DAVIDENKOV and E. L. ASSUR [16] put forward a theory that residual macrostresses are produced during plastic strain as a result of nonuniformity of plastic flow in the surface layers and the core of the test piece. This is due to the mutual constraint on the plastic deformation of cone grains while those crystallites located in surface layers can undergo unconstrained deformation. Such a mechanism of plastic flow results in a higher strain of the surface layers of a tensioned test piece, which gives rise, on unloading, to compressive stresses. The surface layers of a specimen subjected to tension act on core layers, thus generating tensile stresses in the core.

The X-ray method is used to measure the mean value of the macrostress averaged over the volume equal to the product of the cross-sectional area of the original radiation beam by the penetration depth of radiation into the material. The results of measurement of macrostresses discussed in the present paper were obtained by applying nonfiltrated CoKα radiation. The measured quantity was the angular displacement of the 420 line due to the residual macrostress field. The X-ray penetration depth can be assessed by the formula [17]

$$l = K_1 \sin\theta/(2\mu), \tag{4.1}$$

where θ is the Bragg angle and μ — the linear coefficient of absorption of X-radiation.

Assuming, for aluminium, a mass coefficient of absorption $\mu/\varrho = 73.4$ cm^2 g^{-1} [17], we obtain $\mu = \varrho \cdot \mu/\varrho = 198.18$ cm^{-1}. A radiation beam of 99.9% dispersion corresponds to a coefficient $K_1 = 6.91$ [17], therefore 99.9% of the information on the state of stress

originates, under the measurement conditions discussed above, from a depth $l = 172$ μm as computed from Eq. (4.1). Bearing in mind the fact that the penetration depth of X-rays into the material is insignificant, it was assumed that the state of stress is plane at that depth. This enabled us to measure the residual macrostress in the surface layer of a test piece by the method of $\sin^2\psi$ [18]. The dimensions of the radiation beam were 0.25×12 mm. Hexagonal test pieces were used for measuring residual macrostresses. Plane test pieces were cut out from a large specimen (subjected to initial 5% plastic strain) at angles $\alpha = 0$, 30, 60 and 90° with the direction of initial tension. They were 20×100 mm test pieces and were subjected to uniaxial plastic tension to produce a strain of 5%. The results of measurement of the deviation angle γ (Fig. 2) of the direction of the principal tensor of residual macrostress from the direction of the second tensioning is represented in Fig. 8.

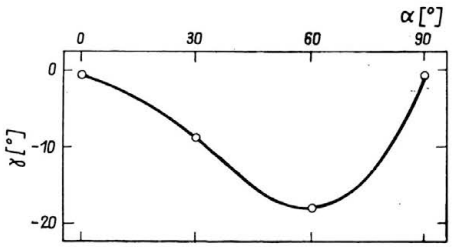

FIG. 8. Variation in the angle γ between the proper direction of the residual macrostress tensor and the direction of secondary plastic strain $\varepsilon_p^{II} = 5\%$ for test pieces cut out at an angle α with the direction of preliminary tension up to $\varepsilon_p^{I} = 5\%$.

5. Experimental investigation into the residual microstress

To investigate the residual microstress due to plastic strain, two 10×100 mm test pieces were cut out from a large test piece (subjected to initial 9.5% plastic strain) at angles $\alpha = 0$, 30, 60 and 90° with the direction of original tension, two for each direction. These test pieces were subjected to uniaxial tension to produce plastic strain as indicated in Figs. 9 to 12. Then residual microstresses were measured. The DRON-2 X-ray diffractometer was used for measurement with filtrated CuKα radiation. The intensity distribution of the lines 111 and 311 was measured. The penetration depth of the radiation into the test piece (assessed in the same manner as it was done in Sect. 4) was 87 μm for the lines 111 and 166 μm for the lines 311. The dimensions of the radiation beam were 0.25×12 mm. The intensity distribution was measured by step-scanning counting of photons. The counting time at a point was 40 seconds, for a step $\Delta 2\theta = 0.05°$ and time the of photon counting at points of the background — 100 seconds. The measurement results were processed by the method of harmonic analysis on an ODRA-1204 computer using a program written by the present author [19]. The values of the microstrains were computed for the crystallographic direction ⟨111⟩ taking a ratio of Young' smoduli $E_{\langle 111\rangle}/E_{\langle 311\rangle} = 1.109$ [19]. The value of Young's moduli were determined for both crystallographic directions making use of the Reuss model. The results of computation of the residual microstrain of the crystal lattice due to plastic strain of a test piece are represented in Figs. 9 to 12 as a function of the multiple of the basic measurement lengths (3.72 μm).

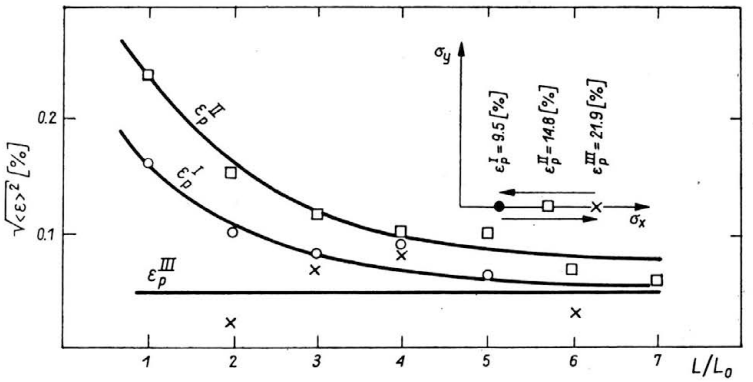

FIG. 9. Variation in the rms microstrains averaged over the length L ($L_0 = 3.72$ nm) for test pieces subjected to plastic strain according to the loading path as shown.

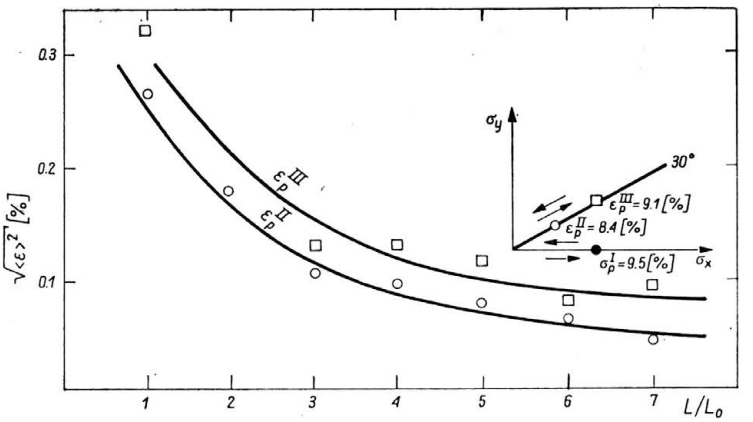

FIG. 10. Variation in the rms microstrains averaged over the length L ($L_0 = 3.72$ nm), subjected to plastic strain along loading path as shown.

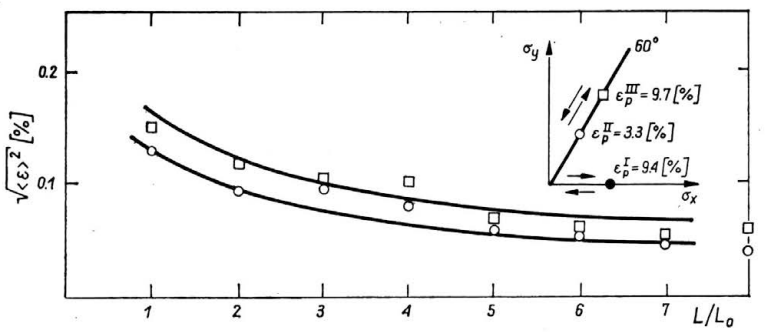

FIG. 11. Variation in the rms microstrains averaged over the length L ($L_0 = 3.72$ nm) length for test-pieces subjected to plastic strain according to the loading path as shown.

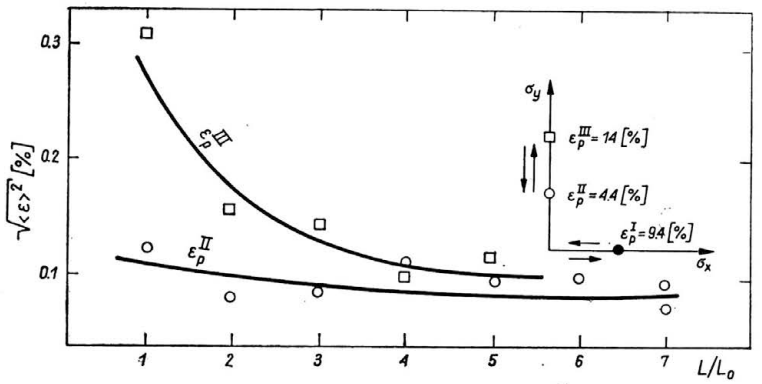

FIG. 12. Variation in the rms microstrains averaged over the length L (L_0 = 3.72 nm), for test pieces subject to plastic strain according to the loading path as shown.

6. Discussion of the results

The results of measurement of variations in principal direction of the plastic strain tensor and the residual macrostress tensor have been presented. The measurement was performed by the grid method and the X-ray technique for residual macrostresses. From Fig. 7 it is seen that the principal directions of the plastic strain tensor lag behind the variation of the directions of the secondary plastic strain produced by tensioning test pieces cut out a plate subjected to previous tension, a measure of the lag being the angle γ, which depends on the direction of the secondary tension and decreases with increasing secondary plastic strain. The principal directions of the residual macrostress tensor lag also behind the direction of secondary strain (Fig. 8). The residual macrostresses were measured in the surface layer of the test pieces. They are equilibrated within the entire cross-section of the specimen, therefore the results concerning the variation of the principal directions may be referred to the entire cross-section. In internal layers of a test piece it is only the sign of the microstress that changes.

Referring to the investigation by W. SZCZEPIŃSKI and J. MIASTKOWSKI [20, 21], the lag in variation of the principal directions of the plastic strain tensor and the residual stress tensor behind the variation of the direction of secondary plastic strain may be interpreted as a memory effect of the material, the strain direction being memorized by a polycrystalline body. The angle γ (Figs. 7 and 8) may be used as a measure of the memory effect of the material.

Figures 9 to 12 represent deformations of the crystal lattice due to plastic strain and produced according to the loading programs represented also in those figures. Figure 9 shows that increased plastic strain produced by uniaxial tension will result in a modified dislocation structure. This is confirmed by a variation of lattice deformations due to plastic strain. For a plastic strain $\varepsilon_p^{II} = 21.9\%$ (Fig. 9) small-angle boundaries are established, what is proved by the character of the variation of lattice deformation as a function of the base length L of measurement. In the case of small-angle boundaries, the relation $\sqrt{\langle\varepsilon\rangle^2} = f(L)$ represents a straight line parallel to the L-axis [22]. From Figs. 10 to 12

it is inferred that repeated tension, at an angle of 30, 60 or 90° with the direction of the initial tension, increases the lattice deformation, the degree of nonhomogeneity being preserved, however, that is $\sqrt{\langle\varepsilon\rangle^2}$ decreases with increasing L.

Figure 13 represents the influence of the plastic strain produced by tension at an angle of 90° with the direction of initial tension on the values of microctresses over a measurement length L = 3.7, 7.4 and 11.1 nm. For smaller values of L the curve of $\sqrt{\langle\varepsilon\rangle^2} - \varepsilon_p^{II}$ has a distinct minimum. The same character of the variation in length show vectors, in the space of stresses, issuing from the origin of coordinates and ending at the line of consecutive positions of the centre of the yield surface, which has been determined experimentally by W. SZCZEPIŃSKI and J. MIASTKOWSKI [20], and J. MIASTKOWSKI [21] for

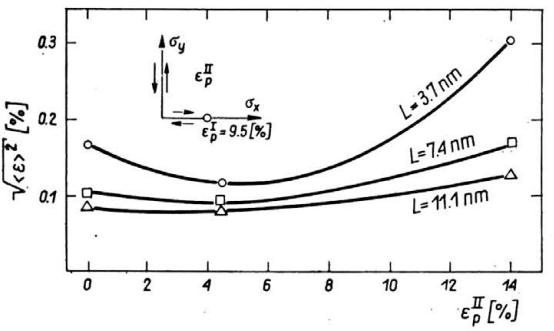

FIG. 13. Variation in the rms microstrains as a function of secondary plastic strain.

plastic strain produced according to the same loading program as in the present paper. In agreement with the idea of kinematic strain hardening developed by W. SZCZEPIŃSKI [23], these vectors represent, in the stress space, residual microstresses. The character of the variation of the residual microstresses determined by measurement as compared with the experimental results obtained by W. SZCZEPIŃSKI and J. MIASTKOWSKI [20] and J. MIASTKOWSKI [21] makes us suppose that the phenomenon of kinematic strain hardening is connected with the presence of residual microstresses.

References

1. A. JU. ISHLINSKY, *General theory of plasticity with linear strain hardening*, Ukr. Matem. Żurn., 3, 314–324, 1954 [in Russian].
2. W. PRAGER, *The theory of plasticity; a survey of recent achievement*, James Clayton Lecture, Proc. Inst. Mech. Engrs., p. 41, 1969 (1955).
3. R. T. SHIELD and H. ZIEGLER, *On Prager's hardening rule*, Zeitschr. Angew. Math. Phys., ZAMP, 19a, 260–275, 1958.
4. JU. I. KADASHEVITCH and V. V. NOVOZHILOV, *Theory of plasticity with consideration of residual microstresses*, Prikl. Matem. Mech., **22**, 78–89, 1958 [in Russian].
5. A. BALTOV and A. SAWCZUK, *A rule of anisotropic hardening*, Acta Mech., **1**, 81, 1965.
6. J. MIASTKOWSKI and W. SZCZEPIŃSKI, *An experimental study of yield surfaces of prestrained brass*, Int. J. Solid Struct., 1, 189–194, 1965.
7. Z. WENDORF, *Metallography*, 482–490, WNT, Warszawa 1976.

8. W. SZCZEPIŃSKI, *On the effect of plastic deformation on yield condition*, Arch. Mech., **15**, 2, 275–296, 1963.
9. G. D. DIEL, *Production mechanics*, Mašinostroj., 41–50, 1978 [in Russian].
10. W. A. KUŹMIENKO, *New schemes for deformation of solids*, Nauk. Dum., 30, Kiev 1973 [in Russian].
11. S. L. SMITH and W. A. WOOD, *A stress-strain curve for the atomic lattice of iron*, Proc. Roy, Soc., A 178, 93–106, 1941.
12. W. A. WOOD and S. L. SMITH, *Stress-strain curve for atomic lattice of aluminium*, Inst. Metals, 67, 909, 315–324, 1941.
13. S. L. SMITH and W. A. WOOD, X-*ray structure and elastic strains in copper*, Proc. Roy. Soc., A 179, 398–411, 1942.
14. S. L. SMITH and W. A. WOOD, *A stress-strain curve for the atomic lattice of mild steel, and the physical significance of the yield point of metal*, Proc. Roy. Soc., A 179, 450–460, 1942.
15. S. L. SMITH and W. A. WOOD, *A stress-strain curve for the atomic lattice of mild steel in compression*, Proc. Roy. Soc., A 181, 72–83, 1942.
16. N. N. DAVIDENKOV, *Mechanical properties of materials and strain measurement methods*, II, Nauk. Dum., 319–323, Kiev 1981 [in Russian].
17. L. I. MIRKIN, *Handbook of* X-*ray analysis of polycrystals*, GIF-ML, 33–38, 1961 [in Russian].
18. T. BRECZKO, X-*ray measurement of residual stress*, Wear, 82, 1, 27–35, 1982.
19. T. BRECZKO, *Calculation of the lattice distortion and the crystallite size*, J. Techn. Phys., 1, 1983.
20. W. SZCZEPIŃSKI and J. MIASTKOWSKI, *An experimental study of the effect of the prestraining history on the yield surfaces of an aluminium alloy*, J. Mech. Phys. Solids, **16**, 153–162, 1968.
21. J. MIASTKOWSKI, *Experimental analysis of the memory effect of a material subjected to plastic strain*, Mech. Teor. Stos., **11**, 3, 297–314, 1973.
22. JA. D. VISHNJAKOV, *Modern methods of investigation into the structure of deformed crystals*, Metall., 348–349, 1975.
23. W. SZCZEPIŃSKI, *On the concept of residual microstresses in plasticity; a more fundamental approach*, Arch. Mech., **32**, 3, 431–443, 1980.

TECHNICAL UNIVERSITY, BIAŁYSTOK.

Received December 6, 1982.